Where are Mars' Hypothesized Ocean Shorelines? Large Lateral and Topographic Offsets Between Different Versions of Paleoshoreline Maps.

Steven F Sholes[1,1], Zachary I Dickeson[2,2], David Montgomery[1,1], and David Catling[1,1]

[1]University of Washington
[2]Natural History Museum

November 30, 2022

Abstract

Mars' controversial hypothesized ocean shorelines have been found to deviate significantly from an expected equipotential surface. While multiple deformation models have been proposed to explain the wide range of elevations, here we show that the historical locations used in the literature and in these models vary widely. We find that the most commonly used version of the Arabia Level does not follow the originally described contact and can deviate laterally by ˜500 km in Deuteronilus Mensae. A meta-analysis of different published maps shows that, globally, the minimum lateral offsets between the locations of the putative Arabia and Deuteronilus shorelines vary by an average of 141±142 km and 180±177 km, respectively. This leads to mean elevations of the Arabia Level that vary by up to 2.2 km between different mappings, and topographic ranges within each global mapping ranging from 2.7 to 7.7 km. The younger Deuteronilus Level has less topographic variation as it largely follows a formal contact (the Vastitas Borealis Formation) within the relatively flat northern plains. Given the high variance in position (spatial and topographic) of the maps, the use of such data and conclusions based on them are potentially problematic.

Where are Mars' Hypothesized Ocean Shorelines? Large Lateral and Topographic Offsets Between Different Versions of Paleoshoreline Maps.

Steven F. Sholes[1,2,3], Zachary I. Dickeson[4,5], David R. Montgomery[1], and David C. Catling[1,2]

[1]Department of Earth and Space Sciences, University of Washington, Seattle, WA, USA.

[2]Astrobiology Program, University of Washington, Seattle, WA, USA.

[3]Jet Propulsion Laboratory, California Institute of Technology, Pasadena, CA, USA

[4]Department of Earth Sciences, Natural History Museum, London, UK.

[5]Department of Earth and Planetary Sciences, Birkbeck College, University of London, London, UK.

Corresponding author: Steven F. Sholes (sfsholes@uw.edu)

Key Points:

- Remapping segments of the putative Mars shorelines finds modern interpolated maps diverge up to 500 km from original geomorphic maps.
- Published maps of the Arabia and Deuteronilus Levels have similar mean lateral offsets of 140 km and 180 km with 1,000 km max offsets.
- A large portion of the topographic disparity of the Arabia Level may be explained through these inconsistent mappings over time.

Abstract

Mars' controversial hypothesized ocean shorelines have been found to deviate significantly from an expected equipotential surface. While multiple deformation models have been proposed to explain the wide range of elevations, here we show that the historical locations used in the literature and in these models vary widely. We find that the most commonly used version of the Arabia Level does not follow the originally described contact and can deviate laterally by ~500 km in Deuteronilus Mensae. A meta-analysis of different published maps shows that, globally, the minimum lateral offsets between the locations of the putative Arabia and Deuteronilus shorelines vary by an average of 141±142 km and 180±177 km, respectively. This leads to mean elevations of the Arabia Level that vary by up to 2.2 km between different mappings, and topographic ranges within each global mapping ranging from 2.7 to 7.7 km. The younger Deuteronilus Level has less topographic variation as it largely follows a formal contact (the Vastitas Borealis Formation) within the relatively flat northern plains. Given the high variance in position (spatial and topographic) of the maps, the use of such data and conclusions based on them are potentially problematic.

Plain Language Summary

Whether oceans ever existed on Mars is controversial, with support largely coming from hypothesized ancient shorelines. As with modern shorelines on Earth, possible ancient martian shorelines are expected to be approximately level, but past studies found that the two main global shoreline mappings have elevation ranges from about one to several kilometers, respectively. Here, we remap segments of the proposed shorelines based on their original geomorphic definitions and find that modern maps vary laterally by hundreds of kilometers from our segments mapped using higher-resolution data. Additionally, we compare maps of potential shorelines over time. We find that maps are both inconsistent and inaccurate with their placement of hypothesized shorelines. Lateral offsets between different maps locally exceed a thousand kilometers. This disagreement with the poorly-understood location of the potential shorelines can explain, in part, the observed elevation differences. Our results question the usefulness of putative shorelines as evidence for ancient martian oceans and implies the need for more detailed, revised mappings and scrutiny.

1 Introduction

Multiple ocean shorelines have been proposed that encircle the northern plains of Mars (Figure 1) but they are controversial (e.g., Carr & Head, 2003; Dickeson & Davis, 2020). Past oceans would imply many constraints on the past climate, habitability, and hydrological evolution of the planet. Putative paleoshorelines have been described as "the most compelling evidence that Mars once had oceans" (Zuber, 2018), but two major problems confront their interpretation: 1) detailed localized geomorphological studies of the putative shorelines consistently find little to no evidence of coastal landforms (e.g., Ghatan & Zimbelman, 2006; Malin & Edgett, 1999; Sholes, 2019; Sholes et al., 2019) contrary to limited studies of south Isidis (Erkeling et al., 2014; Erkeling et al., 2012) and broader regional analyses (e.g., Clifford & Parker, 2001; Parker et al., 1993; Parker et al., 2010; Parker et al., 1989), and 2) the mapped features vary by multiple kilometers in elevation across the planet in contrast to an expected equipotential surface (Carr & Head, 2003) (Figure 2). Here, we set aside the validity of these

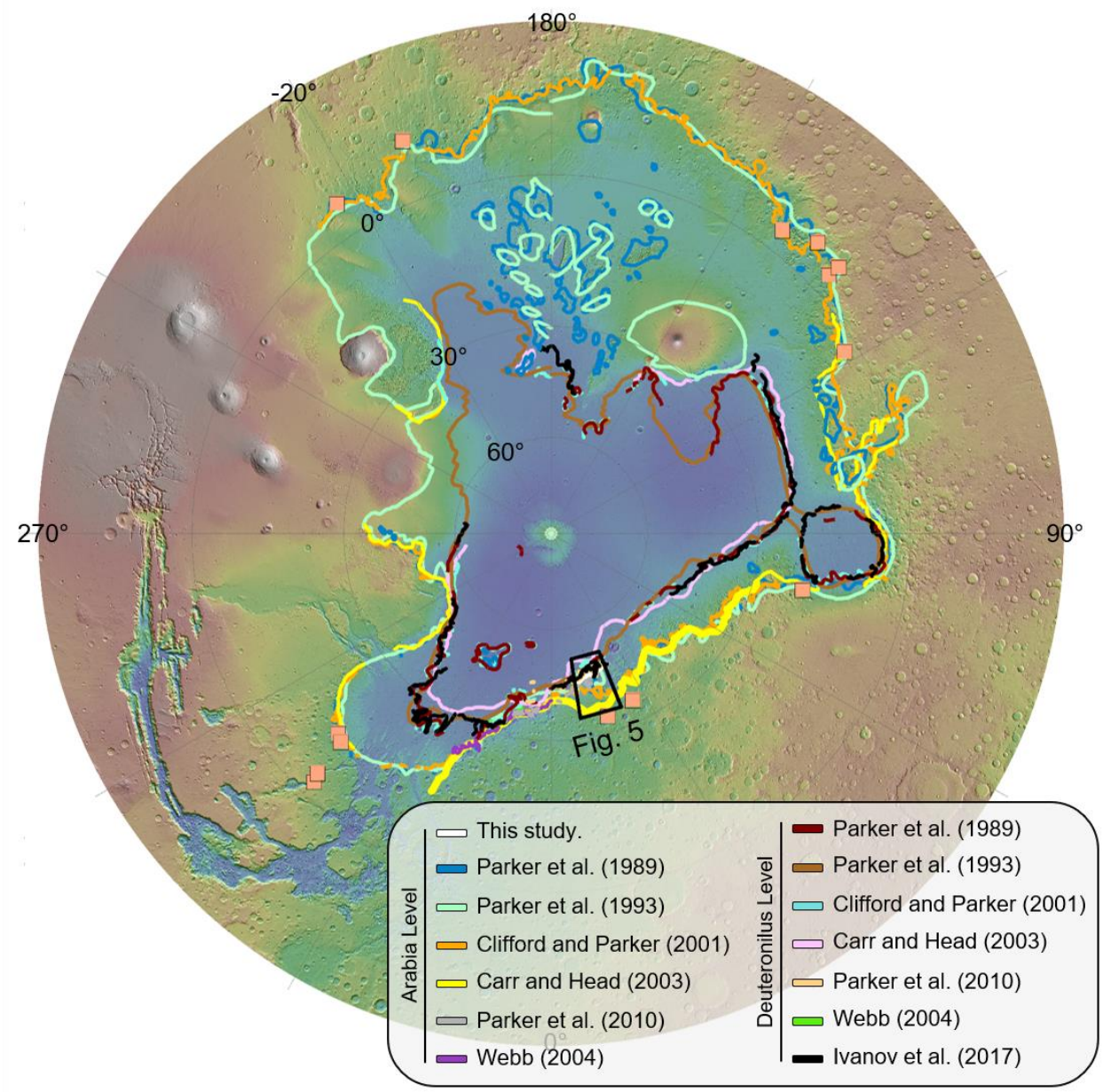

Figure 1: Locations of putative martian shorelines. *a*) Polar stereographic projection showing the composite locations of the Arabia and Deuteronilus Levels as found in various published figures (using MOLA colorized elevation). The bold yellow line indicates the Arabia Level segment from Carr and Head (2003) used in deformation models (e.g., Perron et al. (2007), Citron et al. (2018)). Orange squares are the open deltas from Di Achille and Hynek (2010). Cylindrical projection in Supporting Information (Figure S1).

features as paleoshorelines and, rather, address the mapped locations of the features and how that affects their topographic expression and, by extension, their interpretation.

There are two primary proposed paleoshoreline features, which we hereafter refer to with the non-genetic term "levels," following Parker et al. (2010). These two levels have been mapped to near-complete closure around the northern plains: 1) the Arabia Level ("Contact 1" in the early literature) that roughly follows the topographic dichotomy and has been hypothesized to represent a large early ocean stand; and 2) the Deuteronilus Level ("Contact 2" in the early

literature) which largely follows the southern boundary of the Hesperian-aged Vastitas Borealis Formation (VBF) in the northern plains (Tanaka et al., 2005). Various other levels have been mapped, e.g., the Ismenius, Acidalia, and Meridiani Levels (Edgett & Parker, 1997; Parker et al., 2010), but these are not as thoroughly studied or mapped globally.

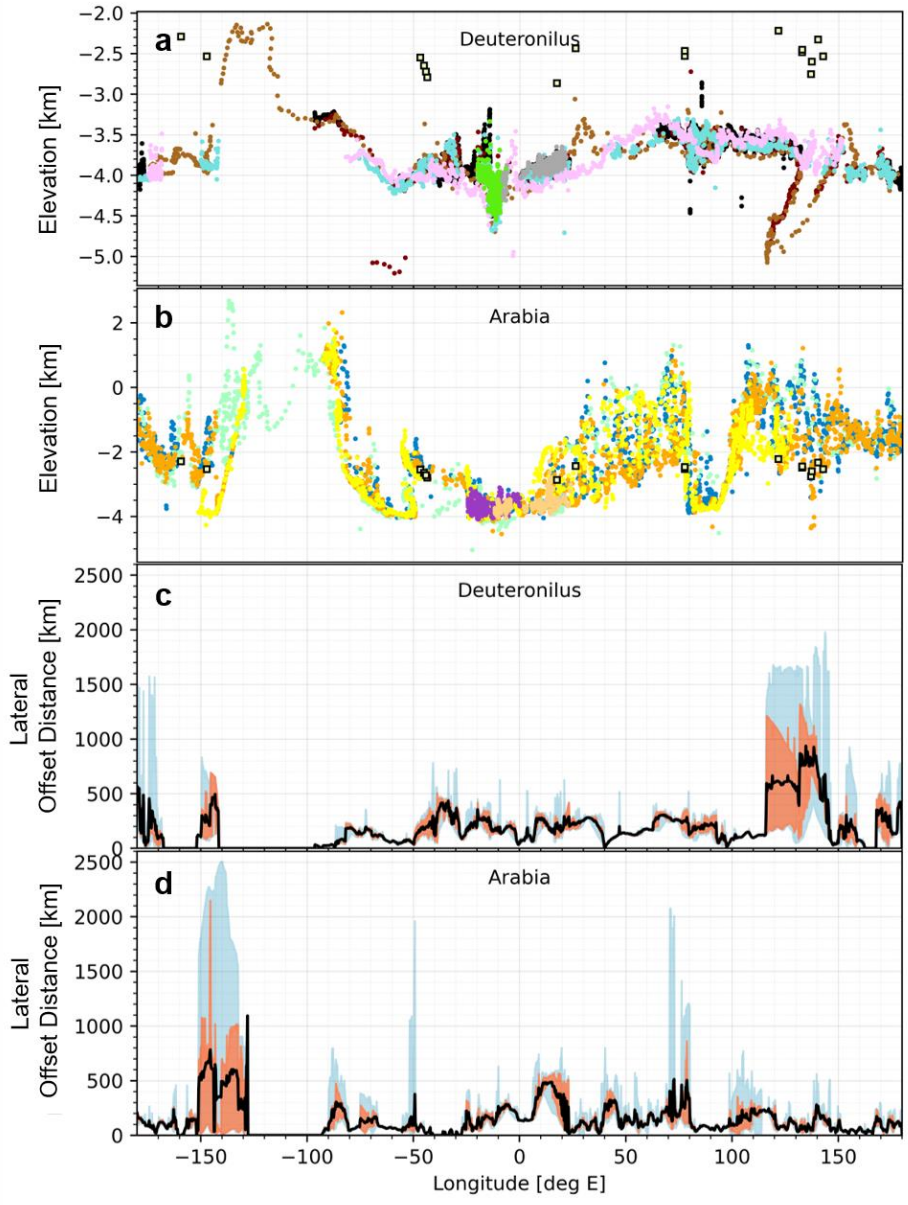

Figure 2: Putative martian paleoshoreline elevations and mean lateral offsets. *a)* and *b)* Topography of the Deuteronilus and Arabia Levels. Di Achille and Hynek (2010) open deltas shown as yellow squares. *c)* and *d)* Mean lateral offsets of the levels (black lines) showing $>10^2$ km discrepancies. Blue shaded region shows the full range of measured offsets across all methods. Red shaded region shows the interquartile range. Statistical summaries of the elevation data in Table 1 and of the offset data in the Supporting Information (Table S1).

While interpretations of these two main hypothesized levels were originally based on a few high-resolution Viking images (~10 m/px) along Mamers Valles, global maps were created predominantly using low-resolution Viking data (>100 m/px) (Parker et al., 1993; Parker et al., 1989). An updated map for both levels was included in Clifford and Parker (2001), which took advantage of a few higher-resolution Mars Orbiter Camera (MOC; Malin & Edgett, 2001) images. Since then, little work has been published to provide updated global maps of the Arabia Level using now-available high-resolution data, e.g., near global coverage at 6-10 m/px with the Context Camera (CTX; Malin et al., 2007). In contrast, the Deuteronilus Level has been updated in a global map by Ivanov et al. (2017) using Thermal Emission Imaging System (THEMIS) infrared (IR) daytime mosaics at ~100 m/px (Christensen et al., 2004).

Absolute elevations of the levels were first analyzed in detail by Head et al. (1999); (1998) using limited Mars Orbiter Laster Altimeter (MOLA) data (Smith et al., 2001), and later expanded on by Carr and Head (2003). The Deuteronilus Level was found to approximate an equipotential surface with a mean elevation of -3.79±0.24 km. While the standard deviation was relatively small, it was not negligible and a total elevation range of 1.2 km was mapped, casting doubt on it representing a paleoequipotential surface. The Arabia Level was found to have a mean elevation of -2.09±1.4 km. With such a large standard deviation, a total range of 5.85 km and lack of convincing geomorphological evidence, the authors largely dismissed the Arabia Level as a possible paleoshoreline, suggesting mass wasting or volcanism as mechanisms for producing the mapped boundary.

Remapping large segments of the Deuteronilus Level by Ivanov et al. (2017) gave an updated mean elevation of -3.76±0.21 km (interdecile range of -4.02 to -3.48 km). However, the authors found that the data were better fit by two distinct regional topographic levels with one area encompassing the Tempe, Chryse, Acidalia, and Cydonia-Deuteronilus regions, having a mean elevation of -3.92 km (interdecile range of -4.01 to -3.83 km), along with the area composed of the Pyramus-Astapus, Utopia, and Western Elysium regions, having a mean elevation of -3.58 km (interdecile range of -3.73 to -3.46 km).

Multiple physical processes have been hypothesized to explain these drastic discrepancies in elevations. Early models invoked isostatic rebound caused by dissipation of the water (Leverington & Ghent, 2004), thermal isostasy (Ruiz et al., 2004), and mantle plumes (Roberts & Zhong, 2004). Later work integrated the mapped levels to argue that true polar wander (TPW; Ivanov et al., 2017; Perron et al., 2007), crustal flexure (Citron et al., 2018), or a combination of the two processes (Chan et al., 2018) could account for the long-wavelength topographic deformation. However, these models are still unable to fully explain the large total spread of elevations along the modeled paleo-topography for the Arabia Level and the results exclude vast sections of the mapped level, only testing against the continuous segment within Arabia Terra.

Variations in the geographic and topographic locations of the levels have also been proposed to be the result of changing sea levels creating smaller regional levels (e.g., the Ismenius and Mamers Valles Levels) (Parker et al., 2010). The possibility of ancient tsunamis and tsunami deposits have also been invoked as means that could obscure or alter potential shorelines, resulting in their possible misidentification or misplacement (Costard et al., 2017; Rodriguez et al., 2016).

Many of the mapped levels currently in use (primarily the Arabia Level and the pre-Ivanov et al. (2017) Deuteronilus Level) stem from vector point data (latitude/longitude) created by Carr and Head (2003) which, in turn, were digitized from the map in Clifford and Parker (2001). This has introduced additional uncertainty as to the exact location of the levels originally identified by Parker et al. and may contribute a substantial portion of the large topographic ranges observed. Problems associated with map projections, line thicknesses, figure resolutions, and sampling points are compounded with the already uncertain position of the levels. Clifford and Parker (2001) note that the levels were "often at the borderline of detectability" and their attempts to correlate them across the planet "invariably led to some misidentifications." The Arabia Level was largely mapped as a series of numerous discontinuous local benches that the authors note may be "manifestations of some other phenomena" rather than coastal terraces. Delineating these benches also proved difficult during the digitization process in Carr and Head (2003), so a smoothed and extrapolated loose fit of the level was mapped instead, especially in Deuteronilus Mensae. Subsequently, we refer to this loose fit of the level as a "regional generalization".

In particular, the Mamers Valles region was used as a type locality for describing the Arabia Level (Parker et al., 1989, their Fig. 4), yet in most maps (primarily those based in part off the Carr and Head (2003) digitization) the level wholly circumvents the Mamers region to the south. This reiterates one of the major underlying problems with the proposed shorelines: whether the observed topographic range is representative of the mapped levels or whether the features are not truly continuous or even marine in origin (Carr & Head, 2019). The lack of publicly accessible georeferenced spatial data for the levels also proves to be a major barrier in studying these features. Here, we quantify variations in how the Arabia and Deuteronilus Levels have been portrayed in maps over time and the associated errors that are caused by data handling, digitization of published maps, and low-resolution mapping.

2 Methods/Data

2.1 Remapping Levels in Deuteronilus Mensae

To test whether published maps of the Arabia Level capture the defining characteristics of the putative paleoshoreline, we remap one of its type localities where features are coherent and observable (located in Deuteronilus Mensae as presented in Parker et al. (1989, their Figure 4b) and again in the Parker et al. (2010, their Figure 9.3) review). The Arabia Level is difficult to map because the level exhibits a range of geomorphic expressions along track and is often discontinuous (Parker et al., 2010; Sholes et al., 2019). For mapping, we use the level description provided in Parker et al. (2010) adapted from Parker et al. (1989, their Figure 4b): a sharp albedo contact between the dark-toned northern plains material and the light-toned upper highlands material. This albedo contrast can be difficult to distinguish in the full-coverage high-resolution CTX imagery, but is apparent in the THEMIS-IR daytime mosaics, so we use a combination of both (i.e., THEMIS IR daytime mosaic overlain with a mosaic of CTX images at 50% opacity). High Resolution Imaging Science Experiment (HiRISE; McEwen et al. (2007)) data is very sparse and insufficient across the boundary and thus not examined here.

Using ArcGIS 10.6 (www.esri.com), we map the entire observable albedo contact (which discontinuously extends for ~800 km) defining the Arabia Level using the layered CTX and THEMIS-IR daytime mosaics across the Deuteronilus Mensae region (see Figure 3). The contact

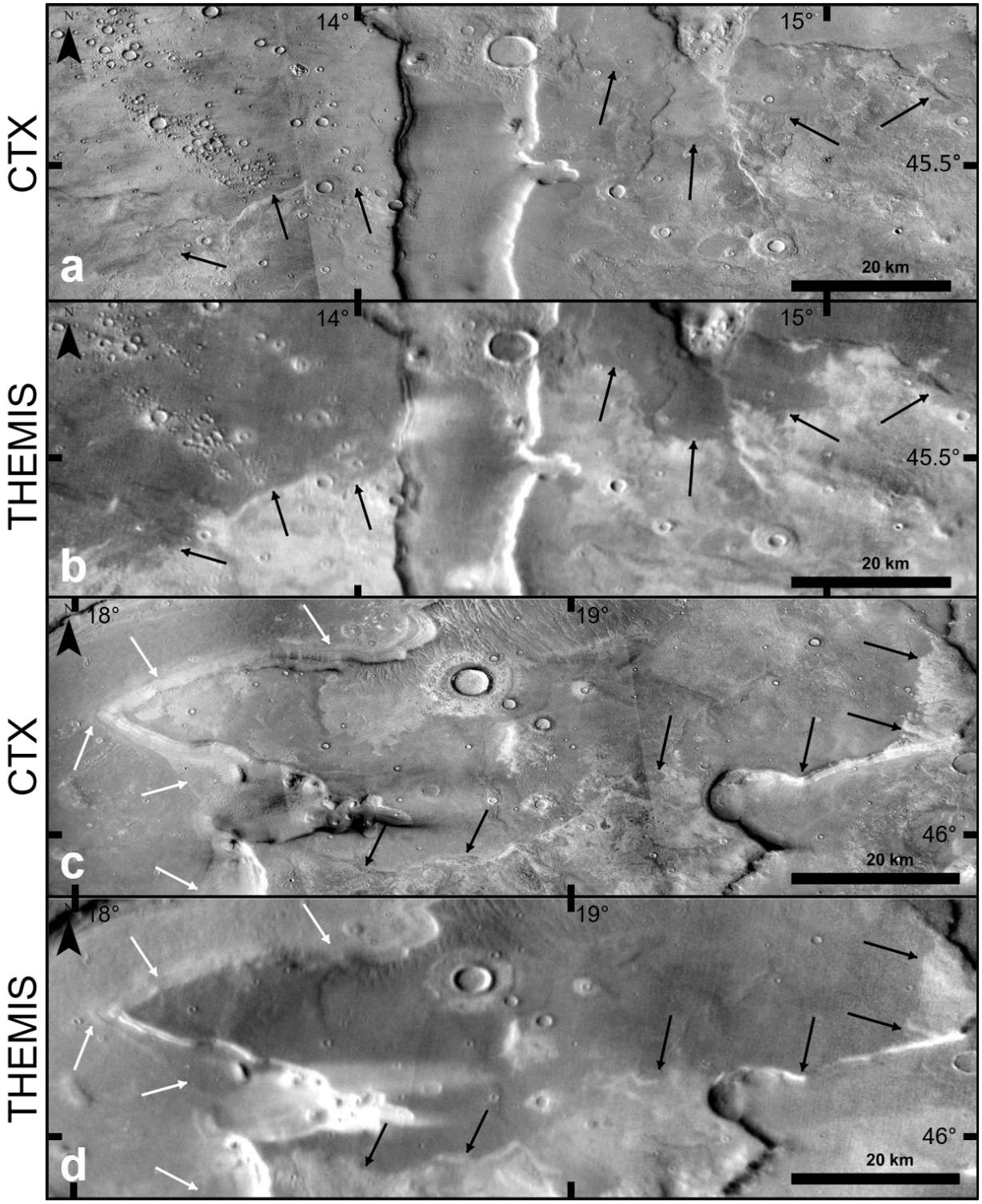

Figure 3: Remapping examples of the Arabia Level within Deuteronilus Mensae. *a*) CTX mosaic of original location used to define the Arabia Level along Mamers Valles. Black arrows indicate location of the contact we map between two distinct units. *b*) THEMIS-IR daytime mosaic of region in *a* showing the distinct albedo contrast used to map the level. *c*) CTX mosaic of a mesa within the dissected terrain that is crosscut by the albedo contact. White arrows indicate the Deuteronilus Level as mapped by Ivanov et al. (2017) and black arrows indicate the contact we use for mapping the Arabia Level. *d*) THEMIS-IR daytime mosaic of *c*. Simple cylindrical projection.

144

is bounded to the east by the Lyot Crater ejecta blanket and to the west by a distinct differently toned dark lowland unit originally mapped as part of the Arabia Level by Parker et al. (1989). However, more recent detailed studies suggest that this contact is the result of localized pooling from catastrophic overland-flow megafloods with no indication of prior standing water (Mangold & Howard, 2013; Sholes, 2019). Thus, we do not include this unit boundary in our mapping.

As we only map the albedo contact where it is distinct and recognizable based on the aforementioned definition, many of the small discontinuous segments included in the Clifford and Parker (2001) map are excluded here. These numerous features are largely proposed small benches and terraces that line the valley walls of the regional dissected terrain, but were noted by the authors to likely be possible manifestations of non-marine processes. These valleys have also been subjected to recent (late Amazonian) glacial modification (e.g., Baker & Head, 2015; Morgan et al., 2009). Levels were not interpolated across gaps where they were either not present (e.g., valleys) or eroded/buried.

We also remap a small representative portion (~350 km) of the Deuteronilus Level ~500 km west of Mamers Valles that had previously been identified as potentially deviating from the Ivanov et al. (2017) mapping (Sholes, 2019). The level was originally mapped primarily with THEMIS-IR daytime mosaics, but we map the Deuteronilus Level (defined largely by the southward-facing lobate flowfronts marking a tonal or textural boundary) using only the high-resolution CTX data to prevent mapping intra-unit contacts that appear as distinct flowfronts in the THEMIS-IR mosaics.

2.2 Global Map Comparisons

To quantify the lateral and topographic variance of the mapped levels globally, we also compare different published versions of the mappings. These maps were chosen to encompass both the primary cited maps and the diversity of relevant published maps labeled as the putative Arabia and Deuteronilius Shorelines (Contacts 1 and 2). Even though maps have been improved upon by the same authors in subsequent later remapping efforts, some more recent studies continue to use the older maps, e.g., basing putative shoreline locations off the original Parker et al. (1989) map instead of the updated Clifford and Parker (2001) map.

Global maps were selected from the following sources: Parker et al. (1989, their Figure 1), Parker et al. (1993, their Figure 1a), and Clifford and Parker (2001, their Figure 6) which all mapped the levels primarily using moderate- to low-resolution Viking data; Carr and Head (2003, their Figure 3) which is a digitization of the map from Clifford and Parker (2001); Ivanov et al. (2017, their Figure 3) mapped the Deuteronilus Level using THEMIS-IR daytime mosaics.

We also include important non-global large-scale regional remappings of the levels. This includes:

- The remapping from this study (Section 2.1, spanning 13° of longitude);
- Webb (2004, their Figures 1 and 4; spanning 25° of longitude) based on unpublished figures from Parker which follow Clifford and Parker (2001). It includes a small remapped segment around the Bamberg Crater ejecta (to maintain an approximate regional equipotential surface);
- Parker et al. (2010, their Figure 9.3; spanning 36° of longitude) which is a segment of the detailed unpublished global remapping by Parker et al.;

- Perron et al. (2007, their Figure 1; spanning 100° of longitude), a segment of the Carr and Head (2003) Arabia Level used in multiple topographic deformation models.

Other studies that examine potential coastal landforms but that did not explicitly map the Arabia or Deuteronilus Levels (beyond comparisons with topographic contours) are excluded (e.g., Erkeling et al., 2012; Ghatan & Zimbelman, 2006). Additionally, we do not include secondary papers that cite the aforementioned data but are not considered mapping efforts (e.g., Fairen et al., 2003; Ormö et al., 2004) along with studies that make paleoshoreline reconstructions not directly ascribed to either the Arabia or Deuteronilus levels (e.g., Fairen et al., 2003; Rodriguez et al., 2016). Many of these studies that provide labeled maps cite both Parker et al. papers (1989, 1993) without providing sufficient details on how the data was obtained (e.g., through digitization, vector files provided by the authors, elevation contours, additional remapping efforts). Furthermore, none of these data are currently archived in any public repositories.

Inquiries were made of many researchers in the community about the availability of vector geospatial files for mapped levels of proposed Mars shorelines (Carr & Head, 2003; Ivanov et al., 2017; Parker et al., 2010; Perron et al., 2007; Webb, 2004). Coordinate points were generously shared by Mikhail Ivanov and Taylor Perron (personal communication) for their respective maps. Where data were not available from the original authors, we digitally traced the levels from the published figures. Each figure image is georeferenced into ArcGIS using the matching projection to ensure projection distortions were not introduced. Figures with no coordinates were georeferenced to major crater centers. A polyline was then manually constructed over the center of each mapped level, with vertices spaced at distances approximate to the line width of the mapped level on the original figure. In this way, the geometry, position, and resolution of each mapped level was replicated in the new vector files.

As with our remapping of Arabia Level in Deuteronilus Mensae, all elevations are compared using the blended MOLA/HRSC (High Resolution Stereo Camera (Jaumann et al., 2007)) elevation model at 200 m/px (Fergason et al., 2018). We do not make any generalizations (as defined earlier) or lateral interpolations of the levels nor do we map the numerous small discontinuous benches such as found in Clifford and Parker (2001).

Quantifying the lateral variance between the various published versions of each level poses a difficult problem due to the complex geometry of the levels as mapped on a spheroid. Here, we consider three main approaches (illustrated in Figure 4):

1) measuring the latitudinal geodesic offsets (i.e., the distance between all mapped levels along a longitudinal cross-section), which is a good approximation of the full offset for sections tracking near latitudinally (east-west),

2) measuring the geodesic distance perpendicular to the mapped levels, which works well at capturing the offsets for sections that do not track latitudinally,

3) using the Haversine formula, which finds the minimum geodetic distance.

Detached “islands” in the northern plains are ignored and offsets are measured at regularly-spaced longitudinal cross-sections (every 0.25°) as the mapped lengths vary greatly.

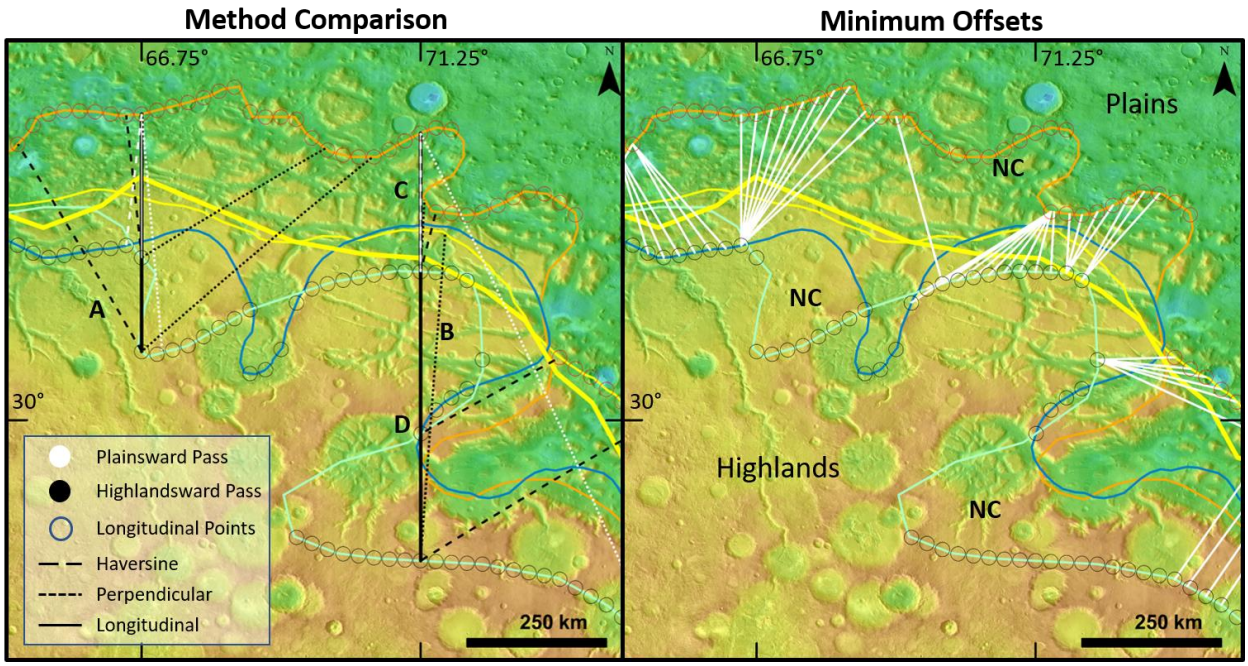

Figure 4: Comparison of offset measuring methodologies and the overall minimum lateral Arabia Level offsets in the Nilosyrtis Mensae region. *Left*) Comparisons of the offsets as measured from two sampled longitudes (66.75° E and 71.25° E). *A* shows how a Haversine offset can be inappropriate as the offset starts from the highlandsward point and extends into the highlands (wrong direction). *B* shows an offset that does not extend across all possible level lines (having already passed through the blue and orange levels). *C* is an example of where multiple offsets are equivalent (Plainsward- and highlandsward- latitudinal and plainsward-Haversine methods). *D* is a highlandsward point where measuring the perpendicular offset is unsuitable as it does not capture all the mapped levels (i.e., misses the yellow levels). *Right*) The minimum offsets for the longitudinal points all end up being Haversine offsets and fail to capture a lot of the offset discrepancies (e.g., non-characterized zones, *NC*). Hence, we present the mean offset between all methodologies and passes. Arabia Level colors same as in Figure 1. MOLA colorized elevation over THEMIS-IR mosaic. Simple cylindrical projection.

Each of these methods has a different set of limitations. Measuring the latitudinal offsets is inadequate for sections that track near-longitudinally (north-south), while measuring perpendicular distances is heavily dependent on the precise large-scale angular geometry of the mapped level. Measuring the minimum Haversine geodetic distance for each point leads to offsets that fail to capture the true geometry of the levels as many sampled longitudinal points along a level segment end up mapping to a single opposing point (Figure 4).

To prevent overestimates, we only map until all regionally cited levels are included. For example, if the levels wrap around features (e.g., craters), the same mapping of a level can appear at multiple spots along the same line of longitude. This highlights the strong dependence offsets have on the chosen level to map from (i.e., if a single mapping is both the northernmost and southernmost point at a given cross-section, measuring the offset between versions starting from the north will be different from starting from the south). Therefore, we measure geodesic offsets following both a plainsward and highlandsward route along track (in contrast to measuring from only the northernmost and southernmost points).

To minimize the influence of these limitations, we take a conservative combined approach by returning the mean offset length between each method and each route (plainsward and highlandsward) at every longitudinal cross-section. We elect to use the mean because the

minimum offset between all methods tends to be dominated by the Haversine function which, as stated above, fails to capture the true geometries of the levels. This combined approach provides a good approximation at quantifying the lateral offset between the mapped levels and the various nuances each method provides in capturing the complex level geometries.

The Isidis basin is not included in our lateral offset measurements of the Deuteronilus Level. This is because most maps have it disjointed from the northern plains which can lead to grossly overestimated offsets following our methodology. Additionally, crater counting by Ivanov et al. (2017) found distinct ages between the VBF and the "VBF-like" unit occupying the Isidis basin which suggests this regional level is distinct from the Deuteronilus Level.

3 Results & Discussion

3.1 Arabia and Deuteronilus Remapping within Deuteronilus Mensae

We find that the Arabia Level within Deuteronilus Mensae, as mapped using the base definition provided in Parker et al. (1989), deviates by up to 500 km from the maps made by Carr and Head (2003) which have been used in various analyses (e.g., Chan et al., 2018; Citron et al., 2018; Perron et al., 2007). Figure 5 presents a direct comparison between our remapped Arabia Level, the Carr and Head (2003) data, the Clifford and Parker (2001) it was based on (which itself was revised from the Parker et al. (1989, 1993) maps), and the updated Deuteronilus Level coordinate points from Ivanov et al. (2017). This offset is largely the result of the smoothed and extrapolated loose fit of the Arabia Level done by Carr and Head (2003) due to aggregation of the numerous small discontinuous segments (e.g., putative benches and terraces along the valley and mesa walls).

The large offset between the different Arabia Level versions within Deuteronilus Mensae corresponds to an average elevation difference of ~1.1 km (Figure 5). Our remapping of the Arabia Level finds an average elevation of -3.55±0.08 km (with an interdecile range of 200 m), while the Carr and Head (2003) data (provided from Perron et al. (2007)) had a local mean elevation of -2.45±0.52 km (with an interdecile range of 1,180 m). This topographic variability is observed spatially in Figure 3a where the traditional Arabia Level (from Carr & Head, 2003) is positioned further south in the highlands, crosscuts large craters and valley networks, and has a data point spacing resolution of ~50 km. This disparity is further compounded by the fact that the Arabia Level straddles the topographic dichotomy, so even relatively small offsets can lead to greater amounts of elevation differences.

While the Arabia Level exhibits different morphologies (onlapping, gradational contacts, and terraces) (Parker et al., 2010), here it largely coincides with the early Hesperian transitional (eHt) and late Noachian highland (lNh) units (Tanaka et al., 2014) (Figure S1 in Supporting Information). The exception is where the albedo contact crosses the mesas within the dissected terrain. Here, the southern boundary of the contact often follows the southern edges of the mesas, which implies that the mapped segments may only be the current southernmost exposure of these units. Due to erosive processes in the region, the current contact may be unrepresentative of the level's paleotopography.

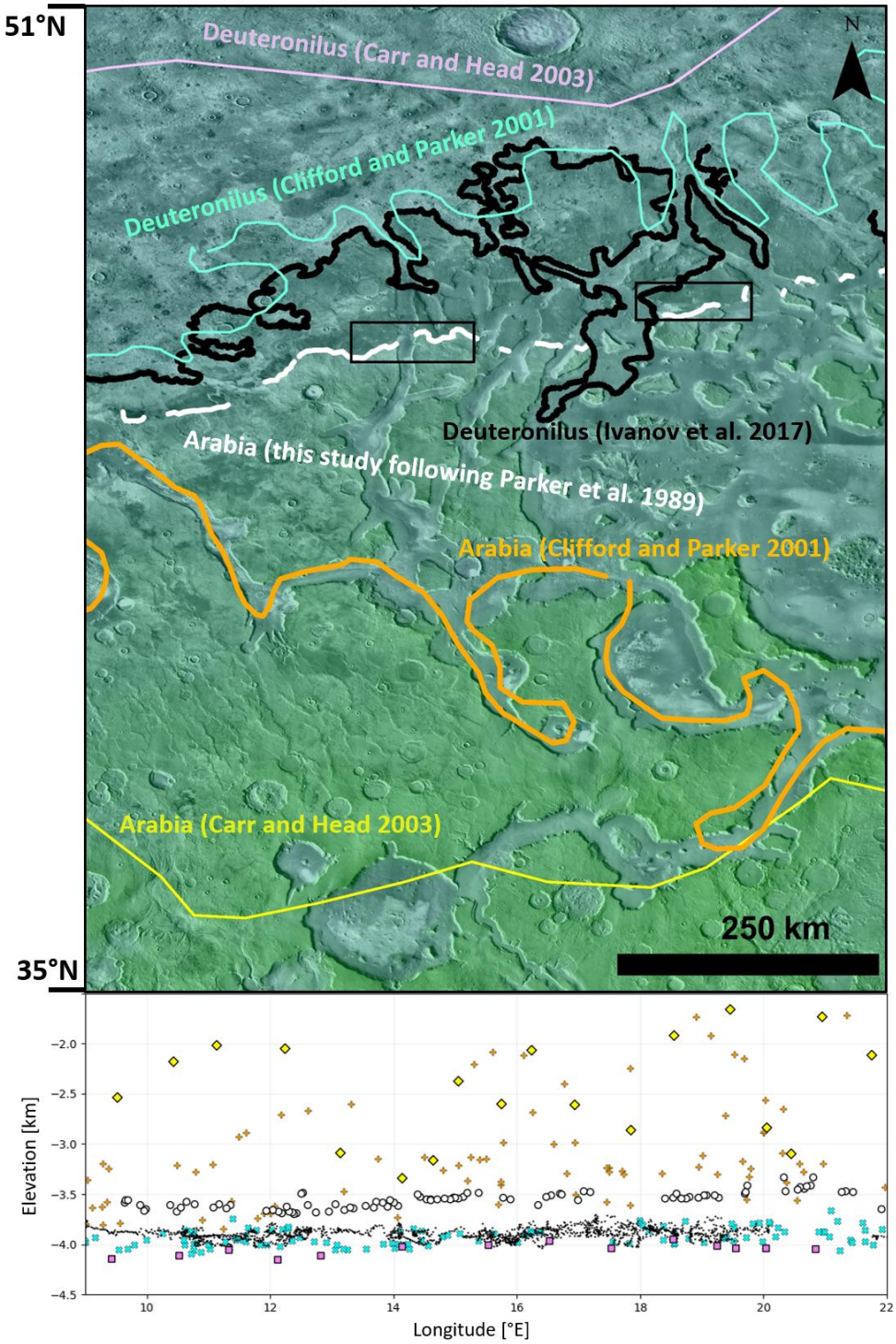

Figure 5: Lateral and topographic variations between different versions of the putative shorelines in Deuteronilus Mensae. *Top*) MOLA colorized elevation over THEMIS-IR daytime mosaic showing the vector data of the Arabia (yellow lines) and Deuteronilus (purple lines) from Carr and Head (2003) along with the Deuteronilus Level from Ivanov et al. (2017) (black lines) and our mapped version of the Arabia Level (white lines) based on the criteria set out in Parker et al. (1989). Our digitized maps of the Arabia (orange lines) and Deuteronilus (cyan lines) from Clifford and Parker (2001) are included. Black boxes indicate areas in Figure 2. Carr and Head (2003) data provided by Perron et al. (2007). *Bottom*) Elevation data corresponding to the levels in the upper panel where the color of each symbol (yellow diamonds, white circles, black dots, purple squares, orange pluses, and cyan crosses) matches the colors and delineated vector data in the upper panel. Simple cylindrical projection.

285

The elevation of the Deuteronilus Level, as remapped by Ivanov et al. (2017), varies by much less than the Arabia Level in this region, even when compared to the old digitized versions, with a topographic offset of ~160 m. This is likely due to the relative flatness of the northern plains (Aharonson et al., 2001; Smith et al., 1998), so even with a maximum lateral offset of ~400 km between the Ivanov et al. (2017) and Carr and Head (2003) maps, the topographic disparity is low.

However, despite the detailed, improved maps made by Ivanov et al. (2017) for the Deuteronilus Level, we find that due to both the resolution of their THEMIS-IR mapping (100 m/px) versus the available CTX data (6-10 m/px) and the variable nature of the VBF that it follows (described below), there are some sections that are incomplete or offset from the base definition. Figure 6 shows the segment of the Deuteronilus Level that we remapped ~500 km west of Mamers Valles (Figure 5) where this offset placement is readily discernible. Here, there are three primary differences in how the level is mapped: *A*) small underlying lobate flows of the VBF that extend beyond the mapped contact; these are virtually indistinguishable in the THEMIS-IR mosaics but pronounced in visual imagery; *B*) sections where the contact is too subtle at THEMIS resolutions. Even with CTX, crater ejecta and other surface processes leave our mapped contact discontinuous in some places; and *C*) erroneously mapped segments that represent intra-unit contacts. While commonly defined as a single unit, the VBF has a range of textural and tonal units throughout (Tanaka et al., 2014; Tanaka et al., 2003; Tanaka et al., 2005). For example, in THEMIS-IR mosaics, Segment C appears to follow the boundary between two distinct light-toned units, but in CTX imagery it becomes apparent that this contact separates two variant units of the thumbprint terrain.

Our remapping over a stretch of ~350 km leads to small adjustments in the elevation and location of the mapped levels. The mean elevation between our remapping and that of Ivanov et al. (2017) differs by only 27 m (-3,927 m vs. -3,954 m respectively), while the difference between the total ranges was only 54 m (165 m for our remapping versus 219 m for Ivanov et al. (2017); similarly, the interdecile range differed by only 10 m between the two versions). Locally, the largest offset is caused by the intra-VBF contact mapping which created a 219 m deviation. Compared with the observed differences seen in the Arabia Level, these are inconsequential, but could compound over the global level.

3.2 Global Shoreline Locations

Our meta-analysis of the published maps for the Arabia and Deuteronilus Levels found that while they overall follow the same general path, there are noticeable deviations between them. Despite citing data obtained from the same base maps (Parker et al., 1993, their Figure 1a ; Parker et al., 1989, their Figure 1), there are multiple instances of lateral deviations >300 km from these base maps. The largest offsets occur in Tharsis and primarily depend on whether the mapped level follows the Olympus Mons aureole rather than the shield. Some offsets are the result of more detailed mapping of the offsets around landforms (e.g., craters, mesas, etc.), but larger offsets are generally where longer sections of the level are mapped more plainsward. For example, in the Arabia Terra region the Parker et al. (1993) version is much more plainsward while the (Carr & Head, 2003) version runs much further south into the highlands.

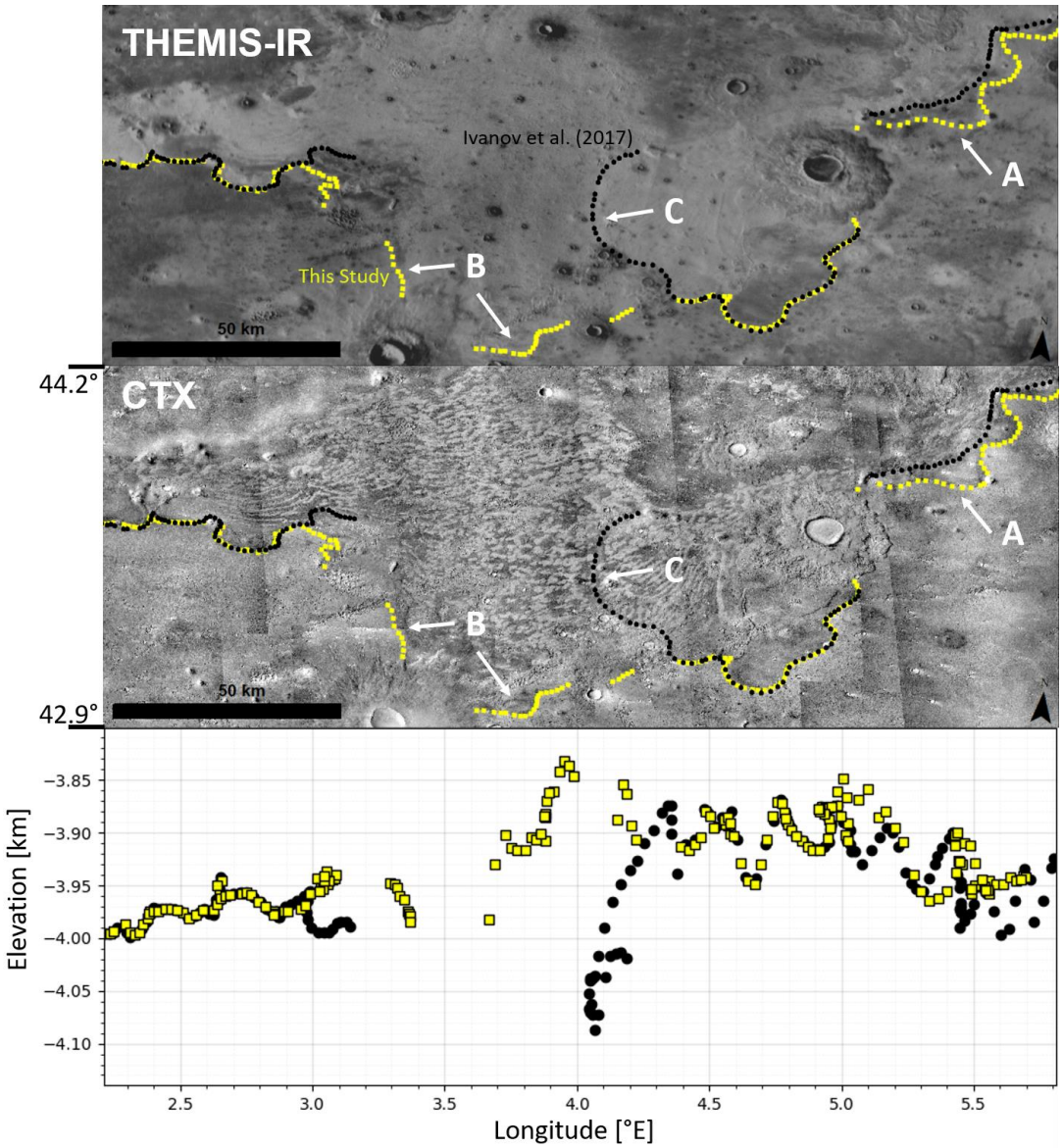

Figure 6: Offsets within the Deuteronilus Level remapping. THEMIS-IR daytime mosaic (*top*) showing Ivanov et al. (2017)'s remapped Deuteronilus Level following the southern boundary of the VBF (black dots) along with our remapped version (yellow squares) using both CTX (*middle*) and THEMIS-IR. *Bottom*: Corresponding elevation data for each of the mapped levels. *A* corresponds to underlying lobate flows that were incorrectly mapped. *B* corresponds to segments that were too subtle to be identified with the THEMIS mosaic. *C* corresponds to an internal contact within the VBF unit. Simple cylindrical projection.

These discrepancies between levels appear to be the result of multiple factors including digitization error, generalizing placement with smoothing and extrapolation, combining data from multiple maps, and redrawing sections based on new interpretations. The availability of MOLA topography also appears to have led to a considerable reinterpretation of previously mapped levels, which were originally mapped based on low-resolution geomorphological or albedo features. The use of different topographical products (e.g., MOLA gridded data at 1/32 degree per pixel versus 1/128 degree per pixel or interpolated MOLA shot points) may also contribute to the elevation variance observed.

Our conservative estimation of the spatial variance of these offsets between all the Arabia Level vector files finds that the different versions vary laterally by an average of 141±142 km globally (Figure 2d) which shows the poorly constrained location of the Arabia Level. The largest deviations (up to 1,093 km) occur along the Olympus Mons aureole. However, most of this region is now largely regarded as no longer a shoreline candidate (Carr & Head, 2003; Clifford & Parker, 2001; Malin & Edgett, 1999), though some have proposed a subaqueous origin for the aureole (De Blasio, 2018).

Similarly, we find the mean minimum lateral offset between global maps of the Deuteronilus Level to be 180±177 km (Figure 2c). The largest offsets occurring within and surrounding Utopia Planitia. However, the Deuteronilus Level has received a recent detailed near-global remapping from Ivanov et al. (2017) and we find that their provided data files closely align with the defining features of the putative paleoshoreline. This is because the Deuteronilus Level is largely defined by a mappable contact (the VBF) unlike the Arabia Level, which additionally has had no such published detailed remapping based on updated higher-resolution data. These results still show a high-degree of uncertainty in the location of the Deuteronilus Level in mappings before Ivanov et al. (2017). Additionally, our results in Section 3.1 show that this mapping is still limited by the resolution and albedo variation of subunits, and is incomplete in places.

The large spatial variance between the different versions of each level contributes to a high degree of uncertainty with the elevation data for each level. Given no standard definition of where the Arabia Level is located, not only is there a large topographic range to the level, but also a large range in the mean elevation across different mappings. The mean elevation between the different Arabia Level versions varies by ~2.2 km: Webb (2004) digitized data have a mean elevation as low as -3.72 km, aligning with previous efforts (e.g., Erkeling et al., 2012; Parker et al., 2010), while Parker et al. (1993) data have it as high as -1.56 km.

The topographic interdecile range within each of the global Arabia Level versions varies from 3.26 km (Clifford & Parker, 2001) to 4.12 km (Parker et al., 1993). These large ranges echo the conclusions of other studies that found a potential ~2 km topographic offset due to the misidentification of the Arabia Level near Apollinaris Patera (Parker & Calef, 2012). However, more detailed regional studies such as provided here, in Webb (2004), and Parker et al. (2010) have much tighter interdecile ranges of 200 m, 450 m, and 610 m respectively. A table of statistics for each of our digitized versions and author-supplied data of the mapped levels is presented in Table 1.

While here we compare the primary mappings (Clifford & Parker, 2001; Parker et al., 1993; Parker et al., 2010; Parker et al., 1989; Webb, 2004) and maps (Carr & Head, 2003) of these putative paleoshorelines prevalent in the literature, it is important to note that further deviations exist among maps that cite these data, often with greater comparable offsets. For example, Ormö et al. (2004, their Figure 1) and Fairen et al. (2003, "Shoreline 2" and the dashed black line in their Figure 2) both cite Parker et al. (1989) and Parker et al. (1993) as their source but diverge from these cited mappings. The Arabia level in Ormö et al. (2004) in particular has a large northward deviation of 350-1,400 km around Alba Mons and an ~700 km eastward offset in north Isidis Planitia not seen in any other mapping of the level. It is unclear why the Arabia level is plotted differently here but may have been done to conceptualize the levels in a very general way especially if the original vector data was not available (personal communication with Jens Ormö and Alberto Fairen). While it is unlikely that other studies would rely on these

secondary maps of the proposed shorelines, it highlights the problem with propagation of variations that can skew results that rely on a known placement of the levels.

Locations of deltas have also been invoked to validate the levels as paleoshorelines, so we also compare their topographic and lateral locations with both Levels (Figure 2). Di Achille and Hynek (2010) proposed a list of 17 open-basin deltas which equated to an ocean level at -2.54±0.18 km. These deltas generally fall along the southern-bounds of the different Arabia Level versions but 6 do not fall within the ranges. Topographically, they all generally fall within the mapped levels, but given the 7.73 km spread of total elevation range across all versions, this is unsurprising. Additionally, detailed higher-resolution studies have found that many of these open deltas fall within localized enclosed basins and have been reinterpreted as forming within paleolakes rather than a northern ocean or sea (Rivera-Hernandez & Palucis, 2019). The locations of valley network termini have also been used in support of a modified (e.g., due to true polar wander or Tharsis loading) paleo-ocean level (Chan et al., 2018).

	Citation	Mean	Standard Deviation	Max	Min	Range	10th Percentile	90th Percentile	Interdecile Range	Length
Arabia	Parker et al. 1989	-1.88	1.22	1.31	-4.03	5.34	-3.63	-0.31	3.32	30,035
	Parker et al. 1993	-1.56	1.54	2.70	-5.03	7.73	-3.68	0.45	4.12	40,630
	Clifford and Parker 2001	-2.19	1.24	2.32	-4.54	6.86	-3.84	-0.58	3.26	39,245
	Carr and Head 2003	-2.31	1.30	1.79	-4.35	6.14	-3.85	-0.58	3.28	16,240
	Webb 2004	-3.72	0.17	-3.12	-4.09	0.96	-3.94	-3.49	0.45	4,765
	Perron et al. 2007*	-2.45	1.23	0.33	-4.10	4.42	-3.84	-0.56	3.28	8,680
	Parker et al. 2010	-3.60	0.26	-2.29	-4.04	1.75	-3.86	-3.26	0.61	2,410
	This Study	-3.56	0.08	-3.33	-3.70	0.37	-3.66	-3.46	0.20	475
Deuteronilus	Parker et al. 1989	-3.86	0.28	-2.72	-5.21	2.49	-4.15	-3.55	0.59	22,845
	Parker et al. 1993	-3.78	0.51	-2.14	-5.07	2.94	-4.28	-3.34	0.94	38,745
	Clifford and Parker 2001	-3.85	0.22	-3.30	-4.67	1.37	-4.09	-3.56	0.53	24,010
	Carr and Head 2003	-3.80	0.26	-3.13	-4.99	1.87	-4.13	-3.47	0.66	18,695
	Webb 2004	-4.12	0.18	-3.30	-4.64	1.34	-4.36	-3.93	0.43	3,580
	Perron et al. 2007*	-3.71	0.27	-3.18	-4.34	1.17	-4.06	-3.39	0.66	16,965
	Parker et al. 2010	-3.90	0.10	-3.65	-4.31	0.66	-4.01	-3.79	0.22	2,370
	Ivanov et al. 2017*	-3.81	0.21	-2.99	-4.42	1.43	-4.04	-3.51	0.53	26,200
	This Study	-3.93	0.04	-3.83	-4.00	0.17	-3.98	-3.88	0.10	250

Table 1: Elevation data, in kilometers, and statistics of the digitized Arabia and Deuteronilus Levels of variable length. Data presented is from our digitization of each map presented in this study, with the exception of those marked by an asterisk (*) where the vector data were provided by the authors. Elevation data uses the MOLA/HRSC elevation map (200 m/px). The Perron et al. (2007) data represents smaller continuous segments of the Carr and Head (2003) digitization. Webb (2004), Parker et al. (2010), and this study are limited regional remappings and isolated "islands" within each map are not included. Ivanov et al. (2017) data excludes the Isidis basin (see text).

4 Conclusions

The Arabia Level, as presented through maps in the published literature, deviates significantly from the location of the proposed definition described originally by Parker et al. (1989). In particular, our investigation of the putative shorelines within the Deuteronilus Mensae region found that the Arabia Level varied by up to ~500 km laterally from traditionally used map data (Carr & Head, 2003), which equates to a regional topographic difference greater than 1.1 km. This substantial offset is the result of the regional generalization of digitized maps and propagation of small variations that stem from this digitization that have continued to this day

due to the lack of publicly available and standardized geographic information system (GIS) file formats for each of the levels.

Furthermore, our global analysis of different maps for the Arabia Level finds that this lateral offset extends globally up to ~1,000 km, with a mean offset of 141±142 km between versions. This large lateral displacement creates a high variance in the elevation of the levels with mean elevations ranging from -1.6 km to -3.7 km and ranges within individual levels up to 7.7 km. Unlike the Deuteronilus Level, which is largely defined by the southern boundary of the VBF, the Arabia Level has no rigorous definition and often exhibits multiple different morphologies making it much more difficult to map in its entirety, further contributing to the wide variance observed.

The Deuteronilus Level was found to have a similar mean lateral offset of 180±177 km between versions. Its location in the relatively flat northern plains creates a much lower variance in the elevation with mean elevations of each level only differing by 0.34 km. Additionally, despite similar offsets to the Arabia Level, the Deuteronilus Level has received a recent detailed remapping by Ivanov et al. (2017). This version is not globally continuous, but more accurately maps the location of the identifiable contact than previous maps.

Historically, the maps used for both discontinuous segments of the Arabia and Deuteronilus Levels have been generalized into smoothed and extrapolated very loose fits (e.g. Carr and Head (2003) in Figure 1), which is insufficient for understanding the true topographic disparity. The Arabia Level is particularly vulnerable to having incorrect elevation because it straddles the topographic dichotomy. Combined with a history of using various versions of digitized maps based on low-resolution Viking imagery, the location of the Arabia Level has much greater uncertainty than the Deuteronilus Level.

The offsets between different versions of the levels are particularly important when trying to assess why they do not meet an expected equipotential surface. Geophysical deformation models have attempted to use these data to explain how long-wavelength processes can create the vast spread in observed elevations of the levels. But, as we have shown, these data can vary drastically from their intended geologic placement. These misplaced and/or misidentified levels will inevitably lead to different results in models that rely directly on the data in their calculations, such determining the TPW paleopole placement in Perron et al. (2007).

Additionally, for the Arabia Level, these models have omitted major mapped portions of the level (e.g., Chan et al., 2018; Citron et al., 2018; Perron et al., 2007), generating uncertainty whether the other mapped segments across the global level follow the same long-wavelength trend. For the Arabia Level in particular, we have also shown that not only is there wide uncertainty in its mapped location, there is a lack of a standardized definition, and large variation in topographic ranges both between and within mapped levels. Thus, caution is warranted when using these data and deriving sweeping conclusions about the history of Mars. The wide variance with the mean elevation and intra-level range can considerably shift the narrative of the timing, extent, and water inventory of such hypothesized oceans.

The interpretation of the margins of the lowland boundaries remains controversial, and is compounded by the uncertainties in mapping laid out in this paper. The Deuteronilus Level has been more rigorously studied, has a narrower topographic range and may be consistent with deposits from an ice- and debris-covered ocean (Carr & Head, 2019; Ivanov et al., 2017; Kreslavsky & Head, 2002; Parker et al., 2010). However, this contact may also be the result of

other processes that are plausible for Mars, such as volcanic, glacial, or subaerial catastrophic flood deposits (Jöns, 1985; Salvatore & Christensen, 2014; Tanaka et al., 2001; Tanaka et al., 2003). The wide topographic and spatial range of the Arabia Level, even when considering the range of different mappings, does not strongly support an ocean hypothesis and may simply be the result of the degradation of the highlands or exposure of different lithological units along the topographic dichotomy (Sholes et al., 2019; Tanaka, 1997).

Overall, the wide displacement between maps of the hypothesized shorelines shows how inaccurate and inconsistent the global mapping of paleoshorelines has been. The Arabia Level maps are particularly poor and require an updated high-resolution global remapping effort fully detailing any global geologic and geomorphic expression (e.g., albedo contacts, terracing, or onlapping relationships). While these results do not preclude the existence of oceans, more compelling evidence is required to support such an interpretation.

Acknowledgments

We thank Mikhail Ivanov and Taylor Perron for graciously sharing their mapped level data along with Serina Diniega, the associate editor Bradley Thomson and three anonymous reviewers who helped improve the clarity of the manuscript. S.F.S. and D.C.C. were partially supported by NASA Astrobiology Institute grant NNA13AA93A. Z.I.D. was partially supported by Science and Technology Facilities Council grant STFC-1967420. The revisions were carried out by S.F.S at the Jet Propulsion Laboratory, California Institute of Technology, under a contract with the National Aeronautics and Space Administration (80NM0018D0004).

Supplemental Data

We provide our mapped and digitized levels as supplemental data which is also archived at doi: 10.5281/zenodo.3743910.

References

Aharonson, O., Zuber, M. T., & Rothman, D. H. (2001). Statistics of Mars' topography from the Mars Orbiter Laser Altimeter: Slopes, correlations, and physical models. *Journal of Geophysical Research: Planets, 106*(E10), 23723-23735. doi:10.1029/2000JE001403

Baker, D. M., & Head, J. W. (2015). Extensive Middle Amazonian mantling of debris aprons and plains in Deuteronilus Mensae, Mars: Implications for the record of mid-latitude glaciation. *Icarus, 260*, 269-288. doi:10.1016/j.icarus.2015.06.036

Carr, M. H., & Head, J. W. (2003). Oceans on Mars: An assessment of the observational evidence and possible fate. *Journal of Geophysical Research: Planets, 108*(E5), 5042. doi:10.1029/2002JE001963

Carr, M. H., & Head, J. W. (2019). Mars: Formation and fate of a frozen Hesperian ocean. *Icarus, 319*, 433-443. doi:10.1016/j.icarus.2018.08.021

Chan, N. H., Perron, J. T., Mitrovica, J. X., & Gomez, N. A. (2018). New Evidence of an Ancient Martian Ocean from the Global Distribution of Valley Networks. *Journal of Geophysical Research: Planets, 123*(8), 2138-2150. doi:10.1029/2018JE005536

Christensen, P. R., Jakosky, B. M., Kieffer, H. H., Malin, M. C., McSween, H. Y., Jr., Nealson, K., et al. (2004). The Thermal Emission Imaging System (THEMIS) for the Mars 2001 Odyssey Mission. *Space Science Reviews, 110*(1-2), 85-130. doi:10.1023/B:SPAC.0000021008.16305.94

Citron, R. I., Manga, M., & Hemingway, D. J. (2018). Timing of oceans on Mars from shoreline deformation. *Nature, 555*(7698), 643-646. doi:10.1038/nature26144

Clifford, S. M., & Parker, T. J. (2001). The Evolution of the Martian Hydrosphere: Implications for the Fate of a Primordial Ocean and the Current State of the Northern Plains. *Icarus, 154*(1), 40-79. doi:10.1006/icar.2001.6671

Costard, F., Séjourné, A., Kelfoun, K., Clifford, S., Lavigne, F., Di Pietro, I., & Bouley, S. (2017). Modeling tsunami propagation and the emplacement of thumbprint terrain in an early Mars ocean. *Journal of Geophysical Research: Planets, 122*(3), 633-649. doi:10.1002/2016JE005230

De Blasio, F. V. (2018). The pristine shape of Olympus Mons on Mars and the subaqueous origin of its aureole deposits. *Icarus, 302*, 44-61. doi:10.1016/j.icarus.2017.11.003

Di Achille, G., & Hynek, B. M. (2010). Ancient ocean on Mars supported by global distribution of deltas and valleys. *Nature Geoscience, 3*(7), 459-463. doi:10.1038/ngeo891

Dickeson, Z. I., & Davis, J. M. (2020). Martian Oceans. *Astronomy & Geophysics, 61*(3), 3.11-13.17. doi:10.1093/astrogeo/ataa038

Edgett, K. S., & Parker, T. J. (1997). Water on early Mars: Possible subaqueous sedimentary deposits covering ancient cratered terrain in western Arabia and Sinus Meridiani. *Geophysical Research Letters, 24*(22), 2897-2900. doi:10.1029/97GL02840

Erkeling, G., Reiss, D., Hiesinger, H., Ivanov, M. A., Hauber, E., & Bernhardt, H. (2014). Landscape formation at the Deuteronilus contact in southern Isidis Planitia, Mars: Implications for an Isidis Sea? *Icarus, 242*, 329-351. doi:10.1016/j.icarus.2014.08.015

Erkeling, G., Reiss, D., Hiesinger, H., Poulet, F., Carter, J., Ivanov, M. A., et al. (2012). Valleys, paleolakes and possible shorelines at the Libya Montes/Isidis boundary: Implications for the hydrologic evolution of Mars. *Icarus, 219*(1), 393-413. doi:10.1016/j.icarus.2012.03.012

Fairen, A. G., Dohm, J. M., Baker, V. R., de Pablo, M. A., Ruiz, J., Ferris, J. C., & Anderson, R. C. (2003). Episodic flood inundations of the northern plains of Mars. *Icarus, 165*(1), 53-67. doi:10.1016/S0019-1035(03)00144-1

Fergason, R. L., Hare, T. M., & Laura, J. (2018). HRSC and MOLA Blended Digital Elevation Model at 200m v2. *USGS Astrogeology Science Center*.

Ghatan, G. J., & Zimbelman, J. R. (2006). Paucity of candidate coastal constructional landforms along proposed shorelines on Mars: Implications for a northern lowlands-filling ocean. *Icarus, 185*(1), 171-196. doi:10.1016/j.icarus.2006.06.007

Head, J. W., Hiesinger, H., Ivanov, M. A., Kreslavsky, M. A., Pratt, S., & Thomson, B. J. (1999). Possible ancient oceans on Mars: evidence from Mars Orbiter Laser Altimeter data. *Science, 286*(5447), 2134-2137. doi:10.1126/science.286.5447.2134

Head, J. W., Kreslavsky, M., Hiesinger, H., Ivanov, M., Pratt, S., Seibert, N., et al. (1998). Oceans in the past history of Mars: Tests for their presence using Mars Orbiter Laser Altimeter (MOLA) data. *Geophysical Research Letters, 25*(24), 4401-4404. doi:10.1029/1998GL900116

Ivanov, M. A., Erkeling, G., Hiesinger, H., Bernhardt, H., & Reiss, D. (2017). Topography of the Deuteronilus contact on Mars: Evidence for an ancient water/mud ocean and long-wavelength topographic readjustments. *Planetary and Space Science, 144*, 49-70. doi:10.1016/j.pss.2017.05.012

Jaumann, R., Neukum, G., Behnke, T., Duxbury, T. C., Eichentopf, K., Flohrer, J., et al. (2007). The high-resolution stereo camera (HRSC) experiment on Mars Express: Instrument aspects and experiment conduct from interplanetary cruise through the nominal mission. *Planetary and Space Science, 55*(7-8), 928-952. doi:10.1016/j.pss.2006.12.003

Jöns, H.-P. (1985). *Late sedimentation and late sediments in the northern lowlands on Mars*. Paper presented at the 16th Lunar Planetary Science Conference, 414-415.

Kreslavsky, M. A., & Head, J. W. (2002). Fate of outflow channel effluents in the northern lowlands of Mars: The Vastitas Borealis Formation as a sublimation residue from frozen ponded bodies of water. *Journal of Geophysical Research, 107*, 5121. doi:10.1029/2001JE001831

Leverington, D., & Ghent, R. (2004). Differential subsidence and rebound in response to changes in water loading on Mars: Possible effects on the geometry of ancient shorelines. *Journal of Geophysical Research: Planets, 109*(E1). doi:10.1029/2003JE002141

Malin, M. C., Bell, J. F., Cantor, B. A., Caplinger, M. A., Calvin, W. M., Clancy, R. T., et al. (2007). Context camera investigation on board the Mars Reconnaissance Orbiter. *Journal of Geophysical Research: Planets, 112*(E5), E05S04. doi:10.1029/2006JE002808

Malin, M. C., & Edgett, K. S. (1999). Oceans or seas in the Martian northern lowlands: High resolution imaging tests of proposed coastlines. *Geophysical Research Letters, 26*(19), 3049-3052. doi:10.1029/1999GL002342

Malin, M. C., & Edgett, K. S. (2001). Mars Global Surveyor Mars Orbiter Camera: Interplanetary cruise through primary mission. *Journal of Geophysical Research: Planets, 106*(E10), 23429-23570. doi:10.1029/2000JE001455

Mangold, N., & Howard, A. D. (2013). Outflow channels with deltaic deposits in Ismenius Lacus, Mars. *Icarus, 226*(1), 385-401. doi:10.1016/j.icarus.2013.05.040

McEwen, A. S., Eliason, E. M., Bergstrom, J. W., Bridges, N. T., Hansen, C. J., Delamere, W. A., et al. (2007). Mars Reconnaissance Orbiter's High Resolution Imaging Science Experiment (HiRISE). *Journal of Geophysical Research: Planets, 112*(E5), E05S02. doi:10.1029/2005JE002605

Morgan, G. A., Head III, J. W., & Marchant, D. R. (2009). Lineated valley fill (LVF) and lobate debris aprons (LDA) in the Deuteronilus Mensae northern dichotomy boundary region, Mars: Constraints on the extent, age and episodicity of Amazonian glacial events. *Icarus, 202*(1), 22-38. doi:10.1016/j.icarus.2009.02.017

Ormö, J., Dohm, J. M., Ferris, J. C., Lepinette, A., & Fairén, A. G. (2004). Marine-target craters on Mars? An assessment study. *Meteoritics & Planetary Science, 39*(2), 333-346. doi:10.1111/j.1945-5100.2004.tb00344.x

Parker, T. J., & Calef, F. J. (2012). *Digital Global Map of Potential Ocean Paleoshorelines on Mars*. Paper presented at the Third Conference on Early Mars, 7085.

Parker, T. J., Gorsline, D. S., Saunders, R. S., Pieri, D. C., & Schneeberger, D. M. (1993). Coastal geomorphology of the Martian northern plains. *Journal of Geophysical Research: Planets, 98*(E6), 11061-11078. doi:10.1029/93JE00618

Parker, T. J., Grant, J. A., & Franklin, B. J. (2010). The northern plains: A Martian oceanic basin? In N. A. Cabrol & E. A. Grin (Eds.), *Lakes on Mars* (pp. 249-273). Boston: Elsevier.

Parker, T. J., Saunders, S. R., & Schneeberger, D. M. (1989). Transitional morphology in West Deuteronilus Mensae, Mars: Implications for modification of the lowland/upland boundary. *Icarus, 82*(1), 111-145. doi:10.1016/0019-1035(89)90027-4

Perron, J. T., Mitrovica, J. X., Manga, M., Matsuyama, I., & Richards, M. A. (2007). Evidence for an ancient martian ocean in the topography of deformed shorelines. *Nature, 447*(7146), 840-843. doi:10.1038/nature05873

Rivera-Hernandez, F., & Palucis, M. C. (2019). Do deltas along the crustal dichotomy boundary of Mars in the Gale crater region record a northern ocean? *Geophysical Research Letters*. doi:10.1029/2019GL083046

Roberts, J. H., & Zhong, S. (2004). Plume-induced topography and geoid anomalies and their implications for the Tharsis rise on Mars. *Journal of Geophysical Research: Planets, 109*(E3). doi:10.1029/2003JE002226

Rodriguez, J. A. P., Fairén, A. G., Tanaka, K. L., Zarroca, M., Linares, R., Platz, T., et al. (2016). Tsunami waves extensively resurfaced the shorelines of an early Martian ocean. *Scientific Reports, 6*, 25106. doi:10.1038/srep25106

583 Ruiz, J., Fairen, A. G., Dohm, J. M., & Tejero, R. (2004). Thermal isostasy and deformation of possible
584 paleoshorelines on Mars. *Planetary and Space Science, 52*(14), 1297-1301. doi:10.1016/j.pss.2004.06.003
585 Salvatore, M. R., & Christensen, P. (2014). On the origin of the vastitas borealis formation in chryse and acidalia
586 planitiae, mars. *Journal of Geophysical Research: Planets, 119*(12), 2437-2456.
587 doi:10.1002/2014JE004682
588 Sholes, S. F. (2019). *Geomorphic and Atmospheric Investigations on the Habitability of Past and Present Mars.*
589 (Doctoral Degree), University of Washington, Seattle, WA.
590 Sholes, S. F., Montgomery, D. R., & Catling, D. C. (2019). Quantitative High-Resolution Reexamination of a
591 Hypothesized Ocean Shoreline in Cydonia Mensae on Mars. *Journal of Geophysical Research: Planets,*
592 *124*(2), 316-336. doi:10.1029/2018JE005837
593 Smith, D. E., Zuber, M., Frey, H., Garvin, J., Head, J., Muhleman, D., et al. (1998). Topography of the northern
594 hemisphere of Mars from the Mars Orbiter Laser Altimeter. *Science, 279*(5357), 1686-1692.
595 doi:10.1126/science.279.5357.1686
596 Smith, D. E., Zuber, M. T., Frey, H. V., Garvin, J. B., Head, J. W., Muhleman, D. O., et al. (2001). Mars Orbiter
597 Laser Altimeter: Experiment summary after the first year of global mapping of Mars. *Journal of*
598 *Geophysical Research: Planets, 106*(E10), 23689-23722. doi:10.1029/2000JE001364
599 Tanaka, K. L. (1997). Sedimentary history and mass flow structures of Chryse and Acidalia Planitiae, Mars. *Journal*
600 *of Geophysical Research: Planets, 102*(E2), 4131-4149. doi:10.1029/96JE02862
601 Tanaka, K. L., Banerdt, W. B., Kargel, J. S., & Hoffman, N. (2001). Huge, CO2-charged debris-flow deposit and
602 tectonic sagging in the northern plains of Mars. *Geology, 29*(5), 427-430. doi:10.1130/0091-
603 7613(2001)029<0427:HCCDFD>2.0.CO;2
604 Tanaka, K. L., Robbins, S. J., Fortezzo, C. M., Skinner, J. A., & Hare, T. M. (2014). The digital global geologic map
605 of Mars: Chronostratigraphic ages, topographic and crater morphologic characteristics, and updated
606 resurfacing history. *Planetary and Space Science, 95*, 11-24. doi:10.1016/j.pss.2013.03.006
607 Tanaka, K. L., Skinner, J. A., Hare, T. M., Joyal, T., & Wenker, A. (2003). Resurfacing history of the northern
608 plains of Mars based on geologic mapping of Mars Global Surveyor data. *Journal of Geophysical*
609 *Research: Planets, 108*(E4). doi:10.1029/2002JE001908
610 Tanaka, K. L., Skinner, J. A., Jr., & Hare, T. M. (Cartographer). (2005). Geologic map of the northern plains of
611 Mars
612 Webb, V. E. (2004). Putative shorelines in northern Arabia Terra, Mars. *Journal of Geophysical Research: Planets,*
613 *109*(E09010). doi:10.1029/2003JE002205
614 Zuber, M. T. (2018). Oceans on Mars formed early. *Nature, 555*, 590-591. doi:10.1038/d41586-018-03415-x
615

Journal of Geophysical Research: Planets

Supporting Information for

Where are Mars' Hypothesized Ocean Shorelines? Large Lateral and Topographic Offsets Between Different Versions of Paleoshoreline Maps.

Steven F. Sholes[1,2,3], Zachary I. Dickeson[4,5], David R. Montgomery[1], and David C. Catling[1,2]

[1]Department of Earth and Space Sciences, University of Washington, Seattle, WA, USA.
[2]Astrobiology Program, University of Washington, Seattle, WA, USA.
[3]Jet Propulsion Laboratory, California Institute of Technology, Pasadena, CA, USA
[4]Department of Earth Sciences, Natural History Museum, London, UK.
[5]Department of Earth and Planetary Sciences, Birkbeck College, University of London, London, UK.

Contents of this file

Introduction

Additional maps to show the full coverage of the mapped levels (Figure S1), provide further insight into the surface geology of the mapped levels (Figure S2), and the differences between the different offset measuring methodologies (Figures S3 and S4). Table S1 summarizes the offset data for each level, method, and pass used. Uploaded separately are comma separated value (.csv) files for each of the mapped levels. These use a polar stereographic Mars projection (north). Elevation data come from the MOLA/HRSC blended digital elevation map at 200 m/px (Fergason et al., 2018). Levels are labeled as First Author + Publication Year + Level + "Z" (for elevation). For example: "Clifford2001_Arabia_Z.csv". Note that elevations from provided geospatial data, i.e., from Ivanov et al. (2017) and Perron et al. (2007), may differ slightly from their respective publications. This is due differing DEMs being used (also explained in the main text).

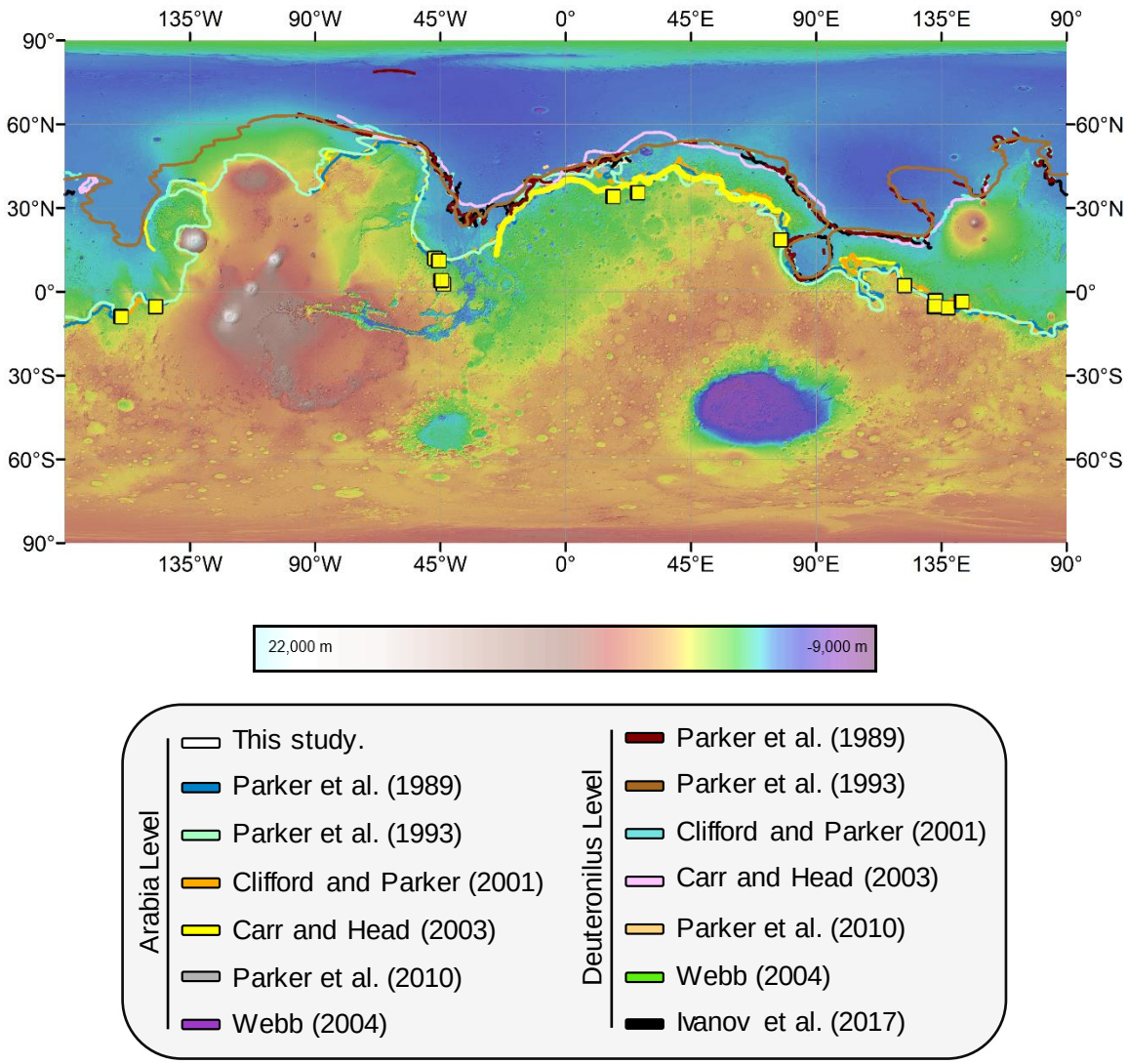

Figure S1. Location of the putative ocean shorelines on a simple cylindrical projection. Yellow squares indicate open deltas from Di Achille and Hynek (2010).

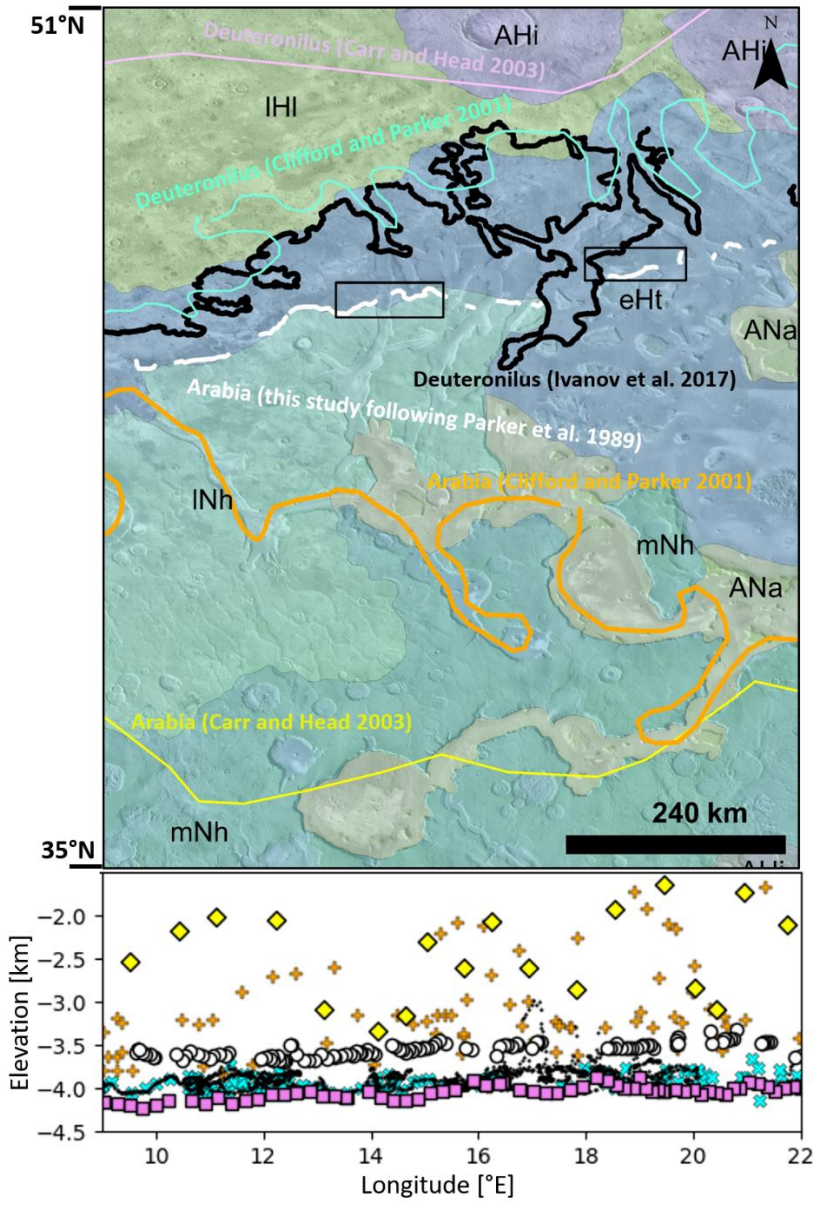

Figure S2. Geological units overlain on Figure 4 (MOLA colorized elevation over THEMIS-IR daytime mosaic). Our mapped Arabia Level (white lines) roughly follows the contact between the early Hesperian transitional (eHt) unit and the late Noachian highlands (lNh) unit. The Deuteronilus Level roughly follows the contact between the eHt and late Hesperian lowlands (lHl) units. mNh: middle Noachian highlands unit, Ana: Amazonian and Noachian apron unit, Ahi: Amazonian and Hesperian impact unit (Tanaka et al., 2014). Colored lines indicate the vector data of the Arabia (yellow lines) and Deuteronilus (purple lines) from Carr and Head (2003) along with the Deuteronilus Level from Ivanov et al. (2017) (black lines) and our mapped version of the Arabia Level (white lines) based on the criteria set out in Parker et al. (1989). Elevation plot for the levels from Figure 3 is reproduced here.

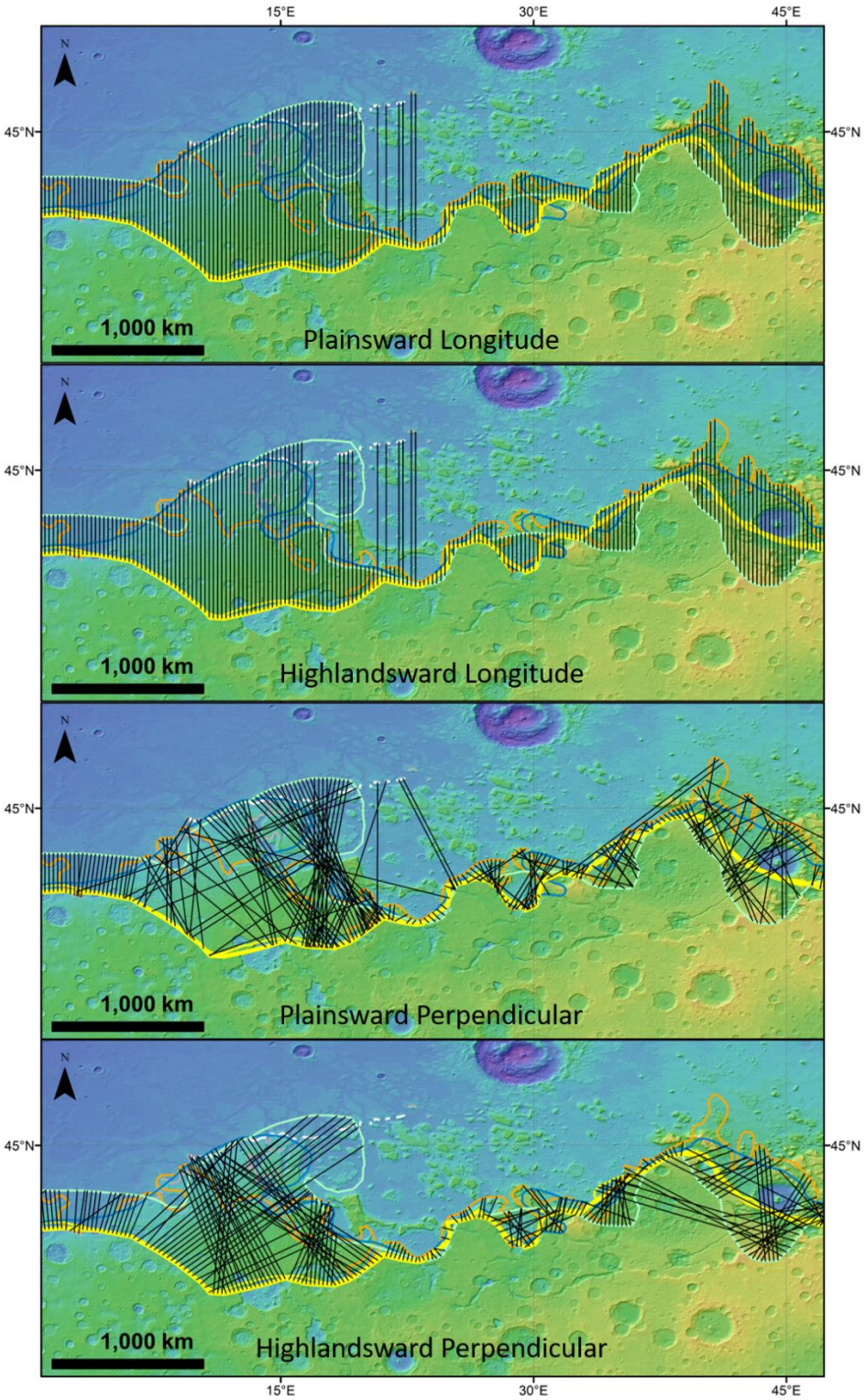

Figure S3: Offsets for the Arabia Level within the Deuteronilus Mensae region for the longitude and perpendicular methods and both the highlandsward and plainsward passes. Simple cylindrical projection.

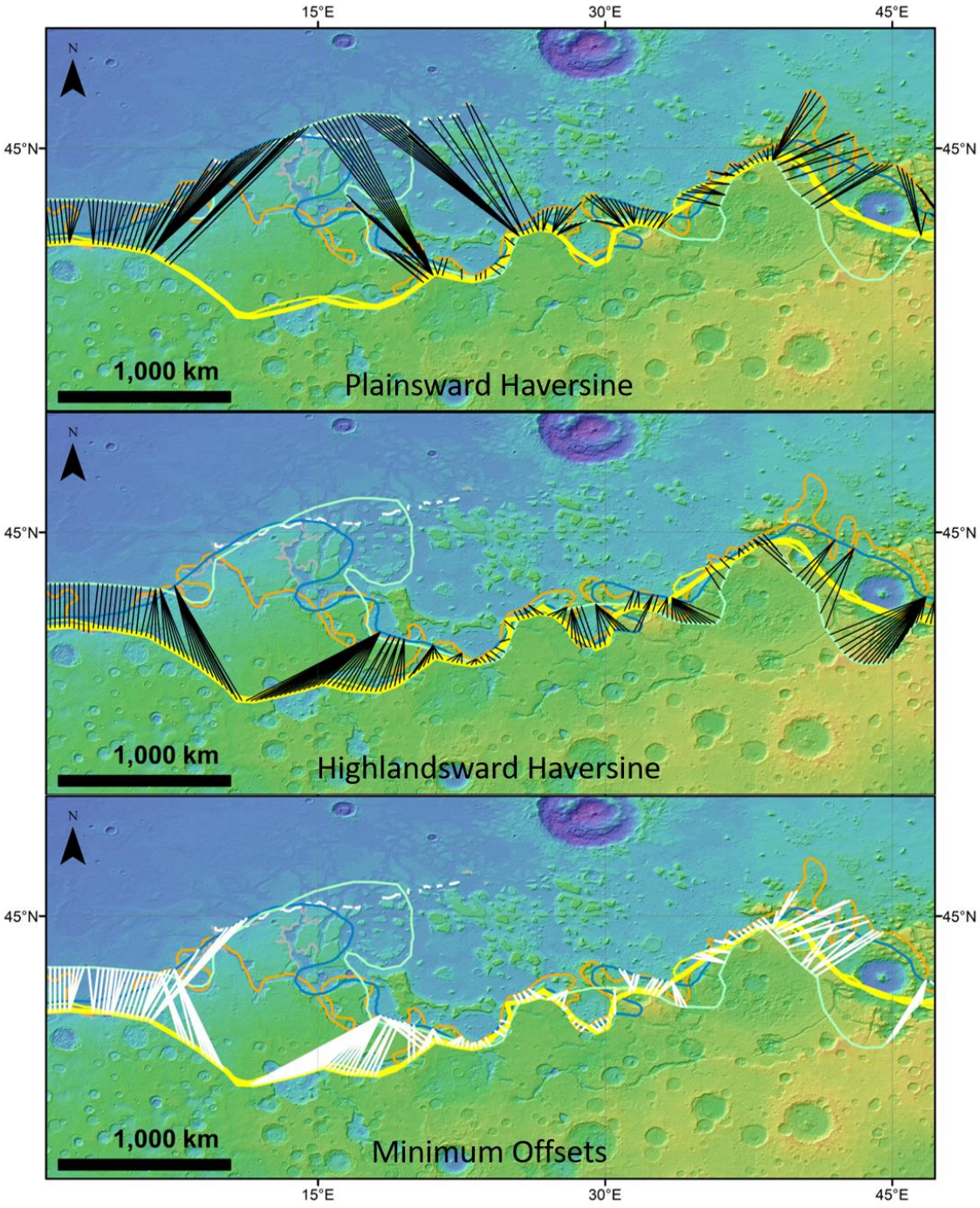

Figure S4: Offsets for the Arabia Level within the Deuteronilus Mensae region for the Haversine function minimization method via both the highlandsward and plainsward passes. Simple cylindrical projection. Minimum offsets figure shows the smallest offset between all methods and passes at each 0.25° longitude. It largely follows the Haversine method but underestimates the overall geometric offsets between all the versions of the levels. The perpendicular method can often overestimate the offsets but can more accurately reflect the offsets when the levels trend roughly longitudinally (N/S).

Table S1. Summary of the different lateral offset distance measurement methods used in the study (all values in kilometers). Offsets are measured in 0.25° longitudinal spacings via both a plainsward-most and highlandsward-most pass. The mean offset ("Mean" method) takes the mean of all available method/pass combinations at each longitude while similarly the minimum offset ("Minimum" method) takes the smallest offset among each method/pass at each longitude. However, due to the nature of the Haversine methods (which finds the minimum distance between each highland point and all plains points, and vice-versa), the minimum offset tends to fail to capture the geometries of the levels themselves and thus the mean offset is a better descriptor of the data.

Level	Method	Pass	Mean	Standard Deviation	Maximum Offset
Arabia	Longitudinal	Highland	269	448	2,506
		Plains	201	332	2,369
	Perpendicular	Highland	162	201	1,458
		Plains	168	221	2,149
	Haversine	Highland	129	164	1,127
		Plains	115	102	647
	Mean	--	141	142	1,093
	Minimum	--	66	67	1,093
Deuteronilus	Longitudinal	Highland	230	189	1,321
		Plains	296	343	1,671
	Perpendicular	Highland	206	206	1,575
		Plains	294	408	1,978
	Haversine	Highland	146	90	455
		Plains	200	216	1,213
	Mean	--	180	177	936
	Minimum	--	95	77	434